

Heterogeneous Catalysis in Solution

Part 25.¹—Contrasting Behaviour of Reduced and Oxidised Platinum Surfaces in the Catalysis of the Reaction Between Cerium(IV) and Mercury(I)

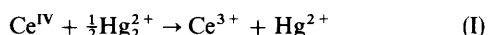
José Manuel Garnica Meza and Michael Spiro*

Department of Chemistry, Imperial College of Science, Technology and Medicine, South Kensington, London SW7 2AY, UK

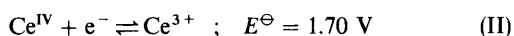
The kinetics of the reaction between Ce^{IV} and Hg_2^{2+} in $1 \text{ mol dm}^{-3} \text{ HClO}_4$ have been studied at 25°C in the presence of a large rotating platinum disc catalyst. When the disc was cathodically preconditioned, the catalytic rate was first order in cerium(IV) and zero order in mercury(I). It was also directly proportional to the square root of the rotation speed and exhibited a low activation energy, which showed that the reaction was mass-transport controlled. There was excellent agreement between the catalytic rate and the limiting current density for Ce^{IV} reduction (converted to rate units by Faraday's law), as would be expected from an electrochemical model of the catalysis. Diffusion coefficients of Ce^{IV} and Hg_2^{2+} in $1 \text{ mol dm}^{-3} \text{ HClO}_4$ were determined from the limiting current measurements. Cyclic voltammetric sweeps after the catalytic runs revealed the presence of underpotential-deposited mercury layers on the platinum surface, and the number of mercury monolayers was evaluated.

In contrast, when the platinum disc was anodically preconditioned, the catalytic rate was smaller, of fractional order in both reactants, and independent of rotation speed. The catalysis was therefore surface-controlled. Kinetic and cyclic voltammetric experiments pointed to the presence of two types of adsorbed mercury species on the oxidised platinum surface which strongly influenced the catalysis. Exposure of the oxidised disc to a solution of Hg_2^{2+} ions before the addition of Ce^{IV} resulted in an increased catalytic rate because the mercury(I) ions had partly reduced the oxidised surface.

The previous two papers in this series have examined the platinum metal catalysis of redox reactions between a positively and a negatively charged species ($\text{Fe}^{3+} + \text{I}^-$)¹ and between two negatively charged species [$\text{Fe}(\text{CN})_6^{3-} + \text{I}^-$].² The present paper reports on catalysis by platinum of a reaction between two highly positively charged ions, namely



Even in the $1 \text{ mol dm}^{-3} \text{ HClO}_4$ medium employed, a considerable percentage of cerium(IV) will have been in the CeOH^{3+} form,³ and the reactant is therefore written as Ce^{IV} throughout. The uncatalysed reaction (I) is extremely slow and photochemically accelerated.⁴ However, in $1 \text{ mol dm}^{-3} \text{ HClO}_4$ at 298 K the standard potentials⁵ of the couples concerned



are far apart, and incomplete information in the literature^{6,7} indicates that both couples are electrochemically reversible. Platinum would therefore be expected to catalyse reaction (I) by an electrochemical mechanism of electron transfer through the metal, a mechanism shown to apply quantitatively in several previous studies.^{1,2,8} In this mechanism the two reactants do not need to sit side by side on the surface (as they do in the Langmuir-Hinshelwood scheme), a particular advantage when the reactants repel each other electrostatically.

The catalysis of reaction (I) by pieces of platinum foil has already been reported by two groups in the literature.^{9,10} Both found that the catalysis was at least partly diffusion controlled, but neither group determined the kinetic orders of the reaction. In order to study the catalysis more quantitatively, we have systematically varied the concentrations of both reactants and products and carefully excluded light, which had been found to affect the homogeneous reaction.⁴ The platinum catalyst was introduced in the form of a large rotating disc. Here the thickness of the Nernst diffusion layer

is given by the modified Levich equation¹¹

$$\delta_i = 0.643 D_i^{1/3} \nu^{1/6} f^{-1/2} P_i \quad (1)$$

where D_i is the tracer diffusion coefficient of reactant i in the medium used, ν is the kinematic viscosity of the solution, and f is the rotation speed. P_i is a small correction factor given by¹²

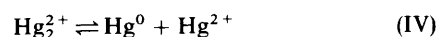
$$P_i = 1 + 0.298(D_i/\nu)^{1/3} + 0.145(D_i/\nu)^{2/3} \quad (2)$$

The rate of diffusion towards the disc is inversely proportional to δ and thus proportional to the square root of the rotation speed f . Since the state of the platinum surface exerted a profound effect on the catalysis, the disc was preconditioned before each run to form either a reduced or an oxidised surface. Cyclic voltammograms and other electrochemical experiments were then carried out on the same surfaces to gain further insight into the catalytic process.

Experimental

Materials

All reagents employed were BDH AnalaR. Stock solutions of $1 \text{ mol dm}^{-3} \text{ HClO}_4$, prepared from the 71% AnalaR reagent, were used as the solvent for the cerium and mercury salt solutions to prevent hydrolysis. Cerium(IV) solutions were prepared from solid $(\text{NH}_4)_2\text{Ce}(\text{NO}_3)_6$ which had been dried at 80°C for 4–6 h¹³ and stored in a desiccator over silica gel. Solutions of cerium(III) and mercury(II) were made by dissolving the $\text{Hg}(\text{NO}_3)_2 \cdot \text{H}_2\text{O}$ and $\text{Ce}(\text{NO}_3)_3 \cdot 6\text{H}_2\text{O}$ salts, respectively. Mercury(I) solutions were prepared by dissolving $\text{Hg}_2(\text{NO}_3)_2 \cdot 2\text{H}_2\text{O}$, recrystallised from dilute nitric acid, in solutions of the mercury(II) salt to avoid the disproportionation reaction



The concentrations of Hg^{I} were determined by titrating these solutions against standard Fe^{III} solutions in the presence of an excess of NaSCN .¹⁴

All solutions were made up with de-ionised Milli-Q water (Millipore) and were stored in the dark. Cerium(IV) and mercury(I)–mercury(II) solutions were prepared and used on the same day.

Electrochemical Experiments

The large rotating platinum disc electrode has been described previously.¹ The sides of the trumpet-shaped brass former were insulated from the solution with four coats of white radiator enamel (International). The platinum surface was regularly hand-polished with $0.3\ \mu\text{m}$ alumina (Banner Scientific). A large platinum foil ($8.5\ \text{cm} \times 8.5\ \text{cm}$) was used as the counter electrode. A saturated sodium chloride calomel electrode (NaSCE) served as reference: it was made by replacing the KCl solution inside a Radiometer K401 calomel electrode with a saturated NaCl solution in order to avoid precipitation of KClO_4 when immersed in the perchlorate solutions. All potentials in this paper are quoted with respect to this electrode. The electrochemical experiments were carried out in a three-compartment cell with a vertical Luggin capillary just below the centre of the rotating disc. Its rotation speed was set with an Oxford Electrodes motor controller. The potentiostat potential was monitored with a Solartron 7045 DMM and the current read with another Solartron DMM across a known resistor. Currents were plotted *vs.* potential or time on a Bryans series 60000 A4 X–Y chart recorder.

The platinum disc was electrochemically cleaned by cycling it at 6 Hz between 0.0 and 1.8 V *vs.* NaSCE in $0.1\ \text{mol dm}^{-3}$ HClO_4 flushed with nitrogen. It was then electrochemically pretreated in $0.1\ \text{mol dm}^{-3}$ HClO_4 by a sequence of three steps. The first two were the same as those recommended by Bruckenstein's group,¹⁵ namely anodisation at 1.84 V at 4.24 Hz for 1 min followed by repeated cycling at $100\ \text{mV s}^{-1}$ between 0 and 1.8 V until reproducible voltammograms were obtained. During this step the electrode was spun momentarily up to 14 Hz as the potential approached 1.3 V during each cathodic scan to remove any oxygen bubbles. Finally, the disc was cathodised at 0 V and 4.24 Hz for 1 min to obtain a reduced surface or anodised at 1.84 V and 4.24 Hz for 1 min to prepare an oxidised surface.

Kinetic Experiments

The catalytic runs were carried out in a two-compartment cell in which a sintered glass frit separated the small reference electrode section from the main reaction compartment of diameter 7.4 cm. The latter was wrapped in black tape to exclude light, and the laboratory lights were switched off during the experiments. The reference compartment was filled with $1\ \text{mol dm}^{-3}$ HClO_4 , and a known volume (typically $200\ \text{cm}^3$) of a solution of one of the reactants in $1\ \text{mol dm}^{-3}$ HClO_4 was placed into the main compartment. After thermal equilibration in the thermostat bath (usually at $25.0 \pm 0.1\ ^\circ\text{C}$), the recently preconditioned platinum disc was lowered into the solution and set to rotate at the required frequency. To start the reaction a small volume (generally $5.00\ \text{cm}^3$) of the second reactant was rapidly pipetted in. For runs with the reduced disc the second reactant was cerium, for those with the oxidised disc it was the $\text{Hg}^{\text{I}} + \text{Hg}^{\text{II}}$ solution. In many later experiments the reactants were mixed first and the platinum disc then lowered to begin the catalytic process. At specific times, samples ($2.5\ \text{cm}^3$) of the reaction mixture were removed and the optical absorbance measured

with a Unicam SP 1800 spectrophotometer at 356 nm where only Ce^{IV} absorbed significantly. Samples were returned to the reaction vessel after analysis, to avoid the need for any volume correction. The absorbance *vs.* time data were later analysed with a microcomputer. The potential difference between the disc and the reference electrode was taken after 15 s (the 'initial' potential) and frequently during the first few minutes of each run as well as at each sampling time. Reactions were generally followed for 1–2 h.

Analytical Methods

The absorbances of cerium(IV) solutions in $1\ \text{mol dm}^{-3}$ HClO_4 at 356 nm followed Beer's law and gave an absorption coefficient ϵ of $507\ \text{dm}^3\ \text{mol}^{-1}\ \text{cm}^{-1}$. Since more nitrate ions were introduced by the mercury salts in the rate studies, absorption coefficients were also determined in the presence of additional NaNO_3 . When the total nitrate ion concentrations were 12.2 and at $28.0\ \text{mmol dm}^{-3}$, ϵ became 578 and $589\ \text{dm}^3\ \text{mol}^{-1}\ \text{cm}^{-1}$, respectively. The appropriate value was used according to the composition of the reaction mixture.

The concentration of mercury(I) in a reaction mixture was determined by a gravimetric method described elsewhere.¹⁶ The presence of platinum ions in the solution was tested for by atomic absorption spectroscopy at 265.9 nm using a Scientific Equipment 6BC 901 instrument. Calibration with 0–50 ppm solutions of BDH Spectrosol platinum chloride in $0.5\ \text{mol dm}^{-3}$ HCl gave a good Beer's law plot.

Results and Discussion

Stoichiometry

A catalytic run with a reduced disc spinning at 9 Hz was carried out at $25\ ^\circ\text{C}$ with $1.0\ \text{mmol dm}^{-3}$ Ce^{IV} , $2.64\ \text{mmol dm}^{-3}$ Hg_2^{2+} and $0.26\ \text{mmol dm}^{-3}$ Hg^{2+} in $1\ \text{mol dm}^{-3}$ HClO_4 . After 2 h the solution was analysed both spectrophotometrically for cerium(IV) and gravimetrically for mercury(I). The resulting losses in the reactants were found to be $5.5 \times 10^{-4}\ \text{mol dm}^{-3}$ in Ce^{IV} and $2.8_3 \times 10^{-4}\ \text{mol dm}^{-3}$ in Hg_2^{2+} . These are in the ratio of 2 : 1.013, which agrees with the expected ratio of 2 : 1 well within the joint experimental error. Reaction (I) therefore retained its stoichiometry under the catalysing conditions. A sample of another catalysed run with a similar initial composition was analysed after 2 h by atomic absorption spectroscopy. No trace of platinum ions was found in the solution, thus proving that the catalyst had not been chemically attacked by cerium ions in the reaction mixture. The possibility of such an attack in the later stages of the run, when the catalyst potential was higher than at the beginning, was not excluded by the Pourbaix diagram for platinum.¹⁷ It was therefore important to test for it since cases of chemical attack on the catalyst being mistaken for heterogeneous catalysis have been documented in the literature.^{8,9}

Catalytic Kinetics with the Reduced Surface

All the kinetic runs were carried out under pseudo-first-order conditions with $[\text{Ce}^{\text{IV}}]_0 \ll [\text{Hg}_2^{2+}]_0$. The kinetic results were accordingly analysed as first order in cerium(IV). Plots of $\ln A$ (where A was the absorbance at 356 nm) against time curved gently downwards and were computer-fitted to the quadratic equation

$$-\ln A = k_0 + k_1 t + k_2 t^2 \quad (3)$$

Table 1 Initial first-order rate constants and catalyst potentials (vs. NaSCE) for the reaction between Ce^{IV} and Hg₂²⁺ in 1 mol dm⁻³ HClO₄ in the dark at 25 °C in the presence of a reduced platinum disc rotating at 9 Hz, unless stated otherwise

run no.	initial concentration/mmol dm ⁻³			E_{cat}/V	$10^6 k_1/\text{s}^{-1}$	comments
	Ce(IV)	Hg ₂ ²⁺	Hg ²⁺			
1-6	1.01	2.53	0.27	0.767	157 ± 7	Ce ^{IV} added to Hg ^I -Hg ^{II} solution immediately after disc immersion
7	1.00	2.51	0.25	0.783	173 ± 3	followed just after run 2
8	1.01	2.50	0.25	0.777 ^a	163 ± 2	1 min disc contact with Hg solution
9	1.00	2.51	0.25	0.819 ^b	165 ± 2	2 h disc contact with Hg solution
10	1.00	2.50	0.29	0.731	157 ± 2	all reagents mixed first
11	0.50	2.54	0.27	0.679	160 ± 3	halved [Ce ^{IV}]
12	2.01	2.49	0.25	0.783	160 ± 2	doubled [Ce ^{IV}]
13	1.02	1.26	0.25	0.769	158 ± 5	halved [Hg ^I]
14	0.99	5.00	0.26	0.726	153 ± 3	doubled [Hg ^I]
15	1.01	2.56	0.52	0.736	167 ± 3	doubled [Hg ^{II}]
16	1.01	2.51	0.00	0.761	163 ± 3	no added Hg ^{II}
17	1.00	2.52	0.28	0.743	160 ± 3	added 0.38 mmol dm ⁻³ Ce ^{III}
18	1.00	2.53	0.26	0.732	160 ± 3	added 10.1 mmol dm ⁻³ NH ₄ NO ₃
19	1.00	2.50	0.24	0.741	110 ± 2	$f = 4$ Hz
20	1.02	2.52	0.26	0.758	218 ± 5	$f = 16$ Hz
21	1.01	2.54	0.25	0.744	213 ± 3	40 °C

^a $E_{\text{cat}} = 0.537$ V at 15 s before Ce^{IV} addition. ^b $E_{\text{cat}} = 0.537$ V at 1 min before Ce^{IV} addition.

The initial rate constants of each run, k_1 , as well as their standard errors of fitting,¹⁸ are listed in Table 1. So are the 'initial' potentials E_{cat} taken up by the platinum disc 15 s after the start of the reaction.

Runs 1-6 were essentially identical catalytic experiments in which k_1 ranged from 1.48×10^{-4} to $1.65 \times 10^{-4} \text{ s}^{-1}$ and E_{cat} from 0.763 to 0.773 V. After the end of run 2 the disc was rinsed with distilled water and then used, without any new preconditioning, as catalyst with a fresh reaction mixture. The somewhat higher rate constant which resulted (run 7) shows that the disc did not lose its catalysing power as the runs proceeded. Runs 8 and 9 demonstrate that longer contact between the disc and the mercury solution before adding the cerium ions had no significant effect on the rate. Nor was a change in rate constant observed in run 10, where the experiment was started by immersing the platinum disc in a previously mixed Ce^{IV} + Hg^I solution. Such a procedure was possible because the homogeneous reaction is very slow in the dark ($k_{\text{hom}} = 2.9 \times 10^{-6} \text{ s}^{-1}$).⁴ Runs 11 and 12, in which the initial cerium concentration was varied by a factor of four, yielded the same rate constant as before, thereby confirming that the reaction was first order in cerium. That it was zero order in mercury(I) was shown by runs 13 and 14, in which a change by a factor of four in the Hg^I concentration did not alter the rate constant. Addition of either of the reaction products, Hg^{II} and Ce^{III}, had no effect on the rate (runs 15-17). The reaction was also insensitive to extra NH₄⁺ and NO₃⁻ ions (run 18) over and above those already present as part of the cerium and mercury salts employed.

The initial kinetics can therefore be represented by the equation

$$-(d[\text{Ce}^{\text{IV}}]/dt)_0 = k_1[\text{Ce}^{\text{IV}}]_0^1[\text{Hg}_2^{2+}]_0^0 \quad (4)$$

with the average rate constant of all the runs at 25 °C and 9 Hz equal to $1.60 \times 10^{-4} \text{ s}^{-1}$. Subtraction of the homogeneous contribution leads to a heterogeneous rate constant k_{het} of $1.57 \times 10^{-4} \text{ s}^{-1}$. A plot of this result and those of the corresponding heterogeneous rate constants at 4 and 16 Hz (runs 19 and 20) against $f^{1/2}$ in Fig. 1 gives a good straight line passing through the origin, a clear demonstration of mass-transport control. Hence

$$k_{\text{het}} = AD_i/V\delta_i \quad (5)$$

where A is the surface area of the platinum disc (10.9 cm²), V the volume of the solution (0.205 dm³), and subscript i stands for Ce^{IV}. Combination of eqn. (1), (2) and (5) leads to

$$k_{\text{het}} = \frac{AD_i^{2/3}v^{-1/6}f^{1/2}}{0.643VP_i} \quad (6)$$

From literature data for the viscosity¹⁹ and density²⁰ of aqueous perchloric acid, the kinematic viscosity of 1 mol dm⁻³ HClO₄ at 25 °C equals $0.8370 \times 10^{-6} \text{ m}^2 \text{ s}^{-1}$. Insertion of the slope of Fig. 1 and the other known parameters then gives $D(\text{Ce}^{\text{IV}}) = 5.25 \times 10^{-10} \text{ m}^2 \text{ s}^{-1}$. The only relevant published tracer diffusion coefficient of Ce^{IV} is that of Greef and Aulich,²¹ who obtained $4.0 \times 10^{-10} \text{ m}^2 \text{ s}^{-1}$ in 1 mol dm⁻³ HClO₄ at 22 °C. These workers also reported a much lower value of ca. $0.7 \times 10^{-10} \text{ m}^2 \text{ s}^{-1}$ at 22 °C in 70% HClO₄ (11.85 mol dm⁻³ HClO₄). This steep decline in $D(\text{Ce}^{\text{IV}})$ with increasing perchloric acid concentration may well be the reason for the 60% decrease in the catalytic rate of reaction (I) observed by Casado *et al.*¹⁰ when they

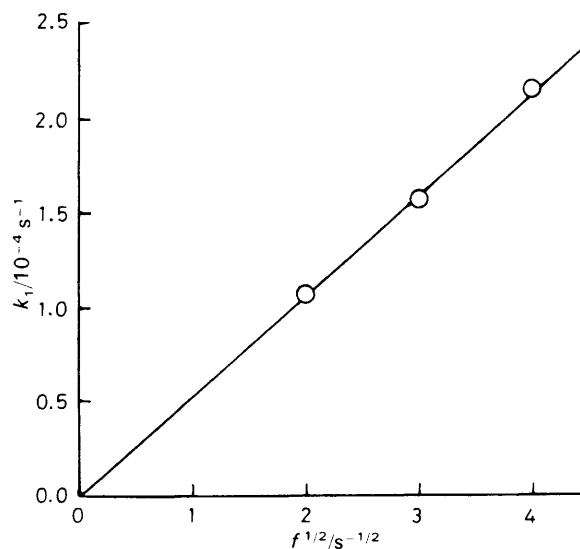


Fig. 1 Dependence of the first-order heterogeneous rate constant at 25 °C on the square root of the rotation speed of the reduced platinum disc

increased the HClO_4 concentration from 0.5 to 2.0 mol dm^{-3} . Both decreases are likely to have been due to changes in Ce^{IV} complexation³ with change of medium, and not to viscosity effects.

A further indication of diffusion control is provided by the activation energy for the catalytic process. At 40 °C and 9 Hz the rate constant was $2.13 \times 10^{-4} \text{ s}^{-1}$ (run 21); subtracting the homogeneous rate constant⁴ of $0.32 \times 10^{-4} \text{ s}^{-1}$ gives $k_{\text{het}} = 1.81 \times 10^{-4} \text{ s}^{-1}$. This leads to an Arrhenius activation energy of $7.7 \pm 1.5 \text{ kJ mol}^{-1}$. The theoretically predicted value for a diffusion-controlled reaction in water between 25 and 40 °C is 15.0 kJ mol^{-1} , as calculated from eqn. (6) and the assumption that the diffusion coefficient obeys the Stokes–Einstein equation with an unchanging hydrodynamic radius. A surface-controlled reaction would be expected to have a significantly higher activation energy. The fact that the value obtained was lower than the predicted one may reflect a change in the effective hydrodynamic radius of Ce^{IV} with temperature.

Electrochemical Experiments with the Individual Couples at the Reduced Surface

Slow-scan (10 mV s^{-1}) current–potential curves were taken of Ce^{IV} solutions in 1 mol dm^{-3} HClO_4 , using the same platinum disc in the form of an electrode. Some of these solutions contained small amounts of added Ce^{3+} . The rest potentials were around 1.4 V, and limiting current plateaux were observed from ca. 1.2 V down to 0.75 V (all with respect to NaSCE). A small degree of hysteresis appeared between the initial cathodic and the subsequent anodic scans; this increased with increasing sweep rate. In order to obtain the tracer diffusion coefficient of Ce^{IV} , limiting currents were measured at 1.00 V at rotation frequencies from 1 to 36 Hz in a solution containing 0.511 mmol dm^{-3} Ce^{IV} , 0.095 mmol dm^{-3} Ce^{3+} and 1 mol dm^{-3} HClO_4 at 25 °C. The plot of I_{lim} vs. $f^{1/2}$ passed close to the origin, but showed a slight downward curvature attributed to gradual oxidation of the platinum surface²¹ as the run proceeded. The values of I_{lim} were therefore computer-fitted to a quadratic in $f^{1/2}$. The initial slope allowed D_i to be calculated according to the equation²²

$$D_i^{2/3} = \frac{0.643v^{1/6}P_i}{nFAc_i} \left(\frac{dI_{\text{lim}}}{df^{1/2}} \right)_0 \quad (7)$$

where i stands for Ce^{IV} , $n = 1$, and F is the Faraday constant. This yielded $D(\text{Ce}^{\text{IV}}) = 5.2_3 \times 10^{-10} \text{ m}^2 \text{ s}^{-1}$, which agrees to better than 1% with the value obtained from the catalytic experiments.

Current–potential curves for Hg^{I} solutions, containing as usual one-tenth as much Hg^{II} , displayed pronounced hysteresis at potentials below the limiting current region, which began above ca. 1.05 V (Fig. 2). The initial anodic sweep on the preconditioned reduced platinum surface was regarded as the relevant curve for present purposes. Limiting currents were measured at 1.35 V in a solution 0.525 mmol dm^{-3} in Hg_2^{2+} and 0.108 mmol dm^{-3} in Hg^{2+} in 1 mol dm^{-3} HClO_4 at 25 °C over rotation speeds from 1 to 36 Hz. The plot of I_{lim} vs. $f^{1/2}$ was a good straight line with a tiny positive intercept. The slope, inserted into eqn. (7) with $n = 2$, gave $D(\text{Hg}_2^{2+}) = 9.7_8 \times 10^{-10} \text{ m}^2 \text{ s}^{-1}$. This figure is close to the values of $9.4 \times 10^{-10} \text{ m}^2 \text{ s}^{-1}$ reported by Hassan *et al.*¹⁵ in 0.1 mol dm^{-3} HClO_4 (at 23 °C?) and $9.3 \times 10^{-10} \text{ m}^2 \text{ s}^{-1}$ obtained by Sluyters–Rehbach and Sluyters²³ in both 0.1 and 1 mol dm^{-3} HClO_4 at 25 °C.

According to the additivity hypothesis of Wagner and Traud,^{24,25} when both the cerium and the mercury couples are present together the disc should adopt a mixture poten-

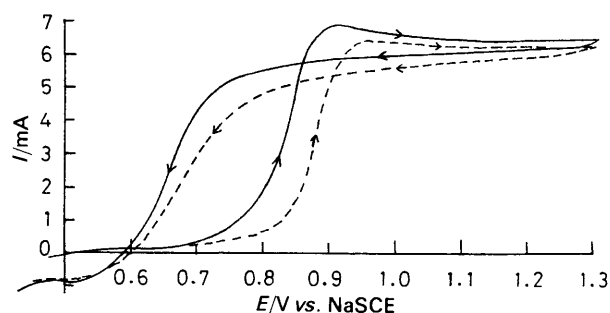


Fig. 2 Current–potential curves of $\text{Hg}^{\text{I}}\text{--Hg}^{\text{II}}$ solutions in 1 mol dm^{-3} HClO_4 at 25 °C taken at 9 Hz at a sweep rate of 10 mV s^{-1} . The full curves refer to a solution of 0.625 mmol dm^{-3} Hg_2^{2+} and 0.064 mmol dm^{-3} Hg^{2+} at a pre-reduced platinum disc, the dashed curves to a solution of 0.664 mmol dm^{-3} Hg_2^{2+} and 0.080 mmol dm^{-3} Hg^{2+} at the disc immediately after the end of run 1 (Table 1)

tial E_{mix} at which the cathodic current due to Ce^{IV} reduction numerically equals the anodic current due to oxidation of Hg_2^{2+} . Plotting the current–potential curves of the two couples on the same sheet of graph paper showed that $E_{\text{mix}} \approx 0.75 \text{ V}$, close to the initial catalyst potentials in Table 1. The electrochemical curves also explain why E_{cat} was lower when the cerium(IV) concentration was halved (run 11) and why it was higher when this concentration was doubled (run 12). All these potentials lie in the limiting current region of Ce^{IV} reduction. Hence, *via* Faraday's law, the surface catalytic rate is given by

$$v_{\text{cat}} = I_{\text{lim}}/FA \quad (8)$$

By eqn. (4) $v_{\text{cat}} = k_{\text{het}}[\text{Ce}^{\text{IV}}]_0 V/A$, which becomes $2.95 \times 10^{-5} \text{ mol m}^{-2} \text{ s}^{-1}$ at the 1 mmol dm^{-3} cerium(IV) concentration used in most of the runs in Table 1. The current–potential curves for 1 mmol dm^{-3} Ce^{IV} gave a limiting current of 3.08 mA, so that $I_{\text{lim}}/FA = 2.93 \times 10^{-5} \text{ mol m}^{-2} \text{ s}^{-1}$. These two independent measurements are therefore in excellent agreement, as predicted by the electrochemical mechanism of the catalysis. It is a natural consequence of this result that the catalytic and the electrochemical experiments furnished virtually identical tracer-diffusion coefficients for Ce^{IV} .

Electrochemical Experiments after Catalytic Runs with the Reduced Surface

Immediately after the end of catalytic run 1 (Table 1), the disc was rinsed with distilled water and immersed in a fresh $\text{Hg}^{\text{I}}\text{--Hg}^{\text{II}}$ solution in 1 mol dm^{-3} HClO_4 at 25 °C. The resulting dashed current–potential curves in Fig. 2 differ from those taken on a freshly preconditioned disc, with the anodic curve after run 1 being shifted to more positive potentials by some 45 mV. The mixture potential would therefore be expected to shift by a similar amount, since the cerium curve remains in the limiting current region throughout. This explains why the potential adopted by the disc during the standard catalytic runs increased with time, the average increase being 41 mV in runs 1, 2, 5 and 6 which had all been followed for 2 h. In run 7, which was conducted with the disc after it had just been used in another catalytic run, the potential was initially higher than before and it actually fell during the experiment. In run 9, where the disc had been in contact with the mercury solution for 2 h before the cerium was added, the initial potential was ca. 50 mV higher than usual, and again there was a fall in E_{cat} during the run.

The cause of the changed behaviour as the runs progressed was investigated by cyclic voltammetry. After run 10 had been followed for 2 h, the disc was rinsed with distilled water

and then immersed in $0.1 \text{ mol dm}^{-3} \text{ HClO}_4$ solution in the three-compartment electrochemical cell. The disc was connected to the potentiostat at 0.56 V and the potential was swept down to 0.0 V , then up to 1.8 V , followed by sweeps between 0 and 1.8 V as in the normal cleaning procedure. In Fig. 3 the first sweep is represented by the full curve and the second sweep by the dashed curve. Two features stand out. First, there is no reduction peak in the first cathodic sweep from 0.56 to 0 V . This means that no platinum 'oxide' (see below) had formed during the run and the pre-reduced surface remained free of oxide throughout, even though the potential at the disc had been large enough to oxidise the surface. However, a typical platinum oxide reduction peak is seen at 0.35 V on the subsequent cathodic sweep. Second, an oxidation peak has appeared at 0.9 V in the first anodic scan. This peak has disappeared in the next and later sweeps, to be replaced by the usual gradual rise due to platinum oxide formation.

The oxidation peak observed only on the first sweep clearly points to a species deposited on the disc during the reaction and oxidised off at a higher potential. A blank experiment was carried out with the reduced platinum disc left in contact with a solution of 0.5 mmol dm^{-3} cerium(IV) and $1 \text{ mol dm}^{-3} \text{ HClO}_4$ for 2 h , rinsed, and swept voltammetrically. A platinum oxide reduction wave appeared on the first sweep showing that the cerium solution had oxidised the platinum surface, but no anodic peak appeared at 0.9 V . Two further blank experiments were then conducted in which the reduced disc was left in contact with a solution of $2.54 \text{ mmol dm}^{-3} \text{ Hg}_2^{2+}$ and $0.23 \text{ mmol dm}^{-3} \text{ Hg}^{2+}$ in $1 \text{ mol dm}^{-3} \text{ HClO}_4$ for 1 min and for 2 h , respectively, rinsed, and immersed in $0.1 \text{ mol dm}^{-3} \text{ HClO}_4$. In both cases oxidation peaks appeared in the first anodic sweep but had disappeared in the second and subsequent anodic sweeps (Fig. 4 and 5). Mercury and not cerium species were therefore responsible for the deposit which produced the oxidation peak observed in Fig. 3 after the catalytic run. This is a clear case of underpotential mercury deposition, since the potential of the platinum disc in run 10 was 0.73 V initially and rising, while the

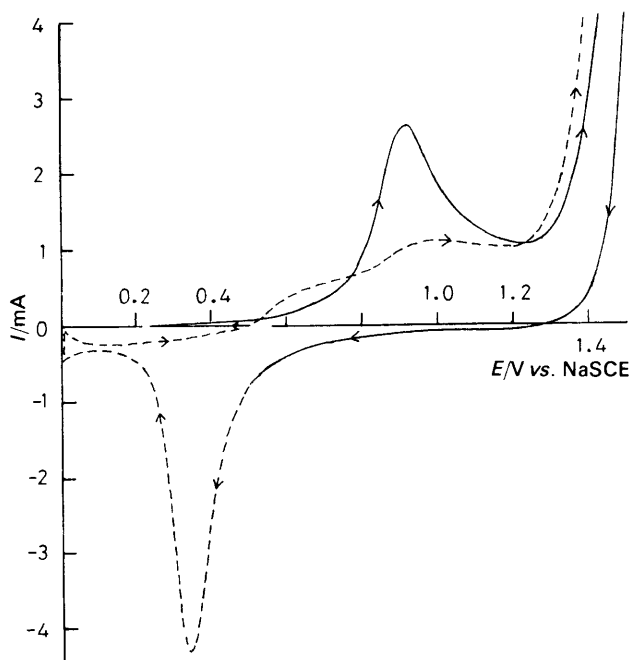


Fig. 3 Voltammetric sweeps of the platinum disc taken immediately after finishing run 10 in Table 1, in $0.1 \text{ mol dm}^{-3} \text{ HClO}_4$ at 25°C at a rotation speed of 6 Hz and a sweep rate of 50 mV s^{-1} . The full curve represents the first sweep and the dashed curve the second sweep

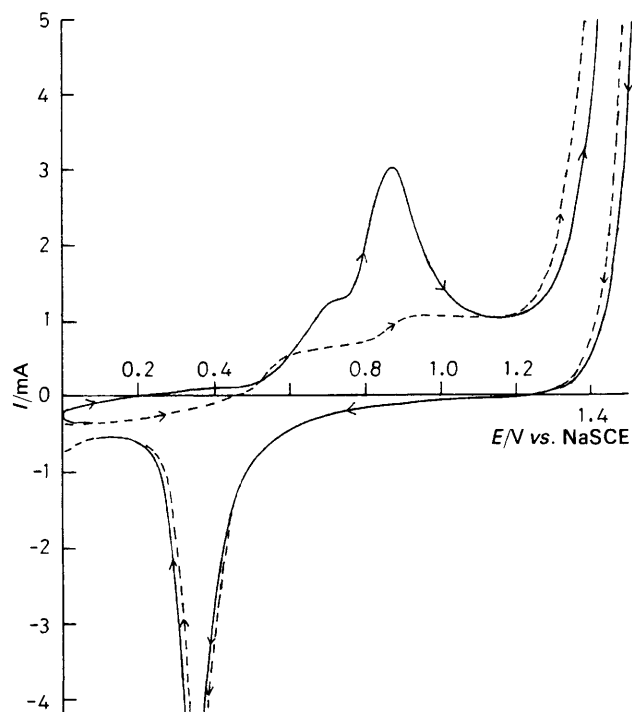


Fig. 4 Voltammetric sweeps of the platinum disc in $0.1 \text{ mol dm}^{-3} \text{ HClO}_4$ at 25°C at 9 Hz and 50 mV s^{-1} , after a 1 min contact between the pre-reduced disc and a solution containing $2.54 \text{ mmol dm}^{-3} \text{ Hg}_2^{2+}$, $0.23 \text{ mmol dm}^{-3} \text{ Hg}^{2+}$ and $1 \text{ mol dm}^{-3} \text{ HClO}_4$. The full curve represents the first sweep and the dashed curve the second sweep

equilibrium potential of the $\text{Hg}_2^{2+}/\text{Hg}$ couple in the solution will have been *ca.* 0.45 V vs. NaSCE . It also follows from Fig. 4 that the deposit is formed within the first minute of mercury-ion contact with the disc. However, while Fig. 3–5 all show a large peak at around 0.9 V , it is preceded in Fig. 4 and 5 by a smaller peak. The latter appears as a shoulder

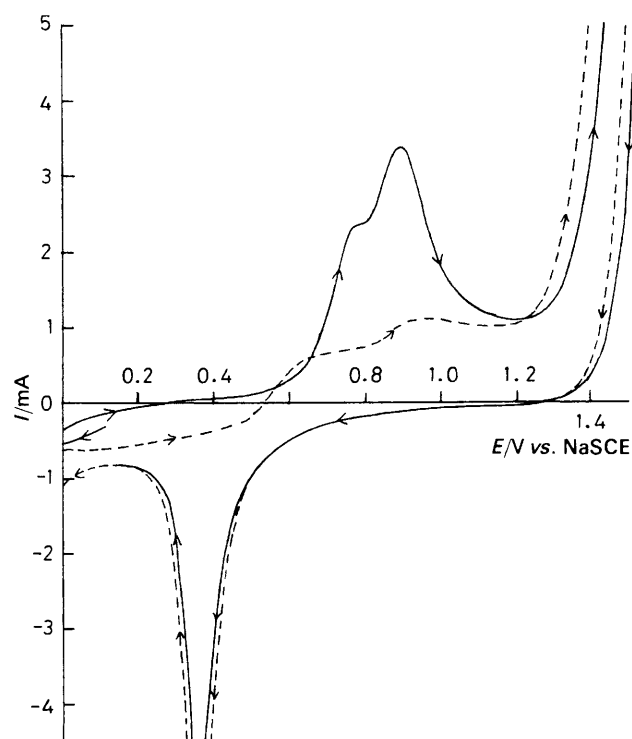


Fig. 5 Voltammetric sweeps of the platinum disc in $0.1 \text{ mol dm}^{-3} \text{ HClO}_4$ at 25°C at 9 Hz and 50 mV s^{-1} , after contact for 2 h between the pre-reduced disc and the same solution as in Fig. 4. The full curve represents the first sweep and the dashed curve the second sweep

which grows in size the longer the disc is in contact with the mercury solution. It also shifts anodically, from *ca.* 0.71 V after 1 min contact to *ca.* 0.79 V after 2 h, as summarised in Table 2.

The deposition of mercury on platinum is a well known phenomenon. Bruckenstein and Hassan²⁶ were the first to show that Hg^I in 1 mol dm⁻³ HClO₄ solution was adsorbed on a reduced platinum electrode. If the electrode was then scanned from the rest potential of 0.49 V *vs.* SCE down to 0.0 V (so reducing Hg^I to Hg⁰) and then up to 1.35 V, a voltammetric peak appeared at 0.9 V in which all the mercury was oxidised to Hg^{II}. This corresponds to the situation in Fig. 3. Subsequently Hassan *et al.*¹⁵ carried out a detailed study in which they observed that the main oxidation peak at 0.9 V was preceded by a smaller peak at *ca.* 0.75 V when more than one monolayer of mercury had been deposited. They ascribed this to the oxidation of a second monolayer of mercury plated on to the first monolayer. At coverages above 2 monolayers the height of the 0.9 V peak decreased while the current between 0.75 and 0.85 V increased until, at around 4 monolayers coverage, the two peaks appeared to merge. These findings accord with the behaviour in Fig. 4 and 5, where the platinum was allowed to remain in progressively longer contact with the disc. Following the procedure of Hassan *et al.*,¹⁵ the areas of the oxidation peaks in these figures were measured and corrected for platinum oxidation by subtracting the areas of the second anodic sweeps under these peaks. The separate areas of the small shoulder peak and of the main peak were also estimated on the assumption that the former is almost symmetrical. The results are listed in Table 2, the area of the disc being taken as 10.9 cm² (*i.e.* a roughness factor of 1). The number of monolayers of mercury was then calculated using the value¹⁵ of 324 μC cm⁻² for the oxidation of one monolayer of Hg⁰ to Hg^{II}.

It can be seen that in run 10 (Fig. 3) some 1.6₃ monolayers of mercury were underpotentially deposited on the platinum

Table 2 Locations of the voltammetric oxidation peaks in Fig. 3–5 and the extents of mercury deposition determined from the areas enclosed

Fig.	peak	position /V (NaSCE)	area /mC cm ⁻²	number of monolayers
3	large	0.92	0.53	1.6 ₃
4	small	0.71	0.13	0.3 ₉ } 2.3 ₃
4	large	0.87	0.63	
5	small	0.79	0.35	1.0 ₇ } 3.2 ₄
5	large	0.89	0.70	

Table 3 Initial rates (with respect to Ce^{IV}) and catalyst potentials (*vs.* NaSCE) for the reaction between Ce^{IV} and Hg₂²⁺ in 1 mol dm⁻³ HClO₄ in the dark at 25 °C in the presence of an oxidised platinum disc rotating at 9 Hz, unless stated otherwise

run no.	initial concentration/mmol dm ⁻³			<i>E</i> _{cat} /V	10 ⁹ <i>v</i> ₀ /mol dm ⁻³ s ⁻¹	comments
	Ce ^{IV}	Hg ₂ ²⁺	Hg ²⁺			
1	1.00	2.51	0.26	0.648	37 ± 2.5	{ Hg ^I -Hg ^{II} added to Ce ^{IV} solution
2	1.01	2.51	0.27	0.651	44 ± 4	
3	1.01	2.50	0.25	0.661	35 ± 2.5	
4	1.01	2.54	0.25	0.686	42 ± 5	after disc immersion all reagents mixed first
5	1.03	2.56	0.22	0.671	46 ± 4	
6	1.00	2.56	0.22	0.694	40 ± 3	<i>f</i> = 4 Hz
7	0.996	2.50	0.26	0.690	28 ± 3	<i>f</i> = 16 Hz
8	0.496	2.51	0.24	0.644	32 ± 3.5	followed just after run 2
9	1.01	4.98	0.24	0.662	47 ± 2	halved [Ce ^{IV}]
10	0.994	2.52	0.25	0.666	47 ± 2	doubled [Hg ^I]
11	1.01	2.53	0.26	0.699 ^a	56 ± 2	added 0.255 mmol dm ⁻³ Ce ³⁺
12	1.01	2.49	0.23	0.808 ^b	57 ± 3	1 min disc contact with Hg solution
					111 ± 2	2 h disc contact with Hg solution

^a *E*_{cat} = 0.544 V at 15 s before Ce^{IV} addition. ^b *E*_{cat} = 0.534 V at 1 min before Ce^{IV} addition.

disc. In this run the reactants were mixed before the disc was immersed. In runs 1–6 in Table 1, where the disc was briefly in contact with the Hg^I + Hg^{II} solution before Ce^{IV} was added, the peak areas in the subsequent cyclic voltammograms were somewhat higher (*e.g.* 1.9₆ monolayers after run 5). Deliberate contact of the disc with the mercury solution for 1 min in run 8 and for 2 h in run 9 led to the formation of 2.3₃ and 3.2₄ monolayers, respectively. As would be expected from the results of Bruckenstein's group, these greater deposits produced two peaks. The ratio of the area of the smaller peak to that of the larger peak more than doubled as the total mercury coverage increased. The heterogeneous catalysis therefore took place on a mercury/platinum surface. On such a surface, as on one of pure platinum, both couples (II) and (III) are likely to be electrochemically reversible,^{6,7} and so both types of surface should catalyse the Ce^{IV} + Hg₂²⁺ reaction by the electrochemical mechanism. The kinetic and electrochemical results bear this out.

The application of this catalysis for analytical purposes has been discussed elsewhere.¹⁶

Catalytic Kinetics with the Oxidised Surface

Analysis of the plots of [Ce^{IV}] against time showed that the reaction here was less than first order in cerium(IV). The initial rates *v*₀, defined by

$$v_0 = - (d[\text{Ce}^{\text{IV}}]/dt)_0 \quad (9)$$

were therefore evaluated by computer-fitting the absorbances to a quadratic in time and taking the initial slopes. The resulting values, together with their standard errors of fitting,¹⁸ are listed in Table 3.

The initial rates of the first three runs average (39 ± 2) × 10⁻⁹ mol dm⁻³ s⁻¹, where the uncertainty limits refer to the average deviation from the mean. These runs had been started by adding the mercury-containing solution to the cerium(IV) solution in which the spinning oxidised disc was already immersed. In run 4 all the reactants were mixed first, and the catalysis was started by lowering the disc into the solution, a procedure justified by the slowness of the homogeneous reaction.⁴ The resulting initial rate agreed with those of runs 1–3 within experimental error, giving an average initial rate for the 4 runs of (39.5 ± 2) × 10⁻⁹ mol dm⁻³ s⁻¹. The volume of the solution was always 0.205 dm³ and the area of the disc 10.9 cm², so that the corresponding areal catalytic rate was (6.9 ± 0.3) × 10⁻⁶ mol m⁻² s⁻¹ after allowing for the homogeneous contribution.⁴ This value is only about one quarter as large as the rate of similar runs with the reduced platinum surface; moreover, the repro-

ducibility was poorer with the oxidised disc. Both these facts point to a surface- rather than a diffusion-controlled catalytic reaction. Confirmation comes from runs 5 and 6, in which the rotation speed of the disc was changed. At 4, 9 and 16 Hz the initial rates were found to be 46, 39.5 and 40×10^{-9} mol dm⁻³ s⁻¹, respectively, thus showing no significant trend with frequency of rotation. The catalytic reaction on the oxidised disc is therefore clearly surface-controlled, in contradistinction to the diffusion-controlled catalysis of reaction (I) on a reduced platinum surface.

To test how the catalytic effectiveness of the surface changed during a run, the disc was rinsed immediately after the completion of run 2 and then inserted into a fresh reaction mixture without any further preconditioning. The resulting rate in run 7 was over 30% smaller than in runs carried out with a freshly conditioned disc. This again differs from the behaviour observed with a reduced platinum surface. Run 7 helps to account for the gradual decline in rate as runs with oxidised discs proceeded. It is worth noting that atomic absorption experiments showed no trace of platinum ions in the solution at the end of a reaction.

The results of runs 8 and 9, using the same procedure as in run 4 but with different concentrations of the reactants, lead to catalytic kinetics which are of fractional order in both Ce^{IV} and Hg₂²⁺. Subtracting the homogeneous contribution to the rate⁴ and making due allowance for the uncertainties in the rates gives

$$v_0 = k_{\text{cat}}[\text{Ce}^{\text{IV}}]_0^x[\text{Hg}_2^{2+}]_0^y \quad (10)$$

where $x = 0.32 \pm 0.22$ and $y = 0.26 \pm 0.12$. Theory based on the electrochemical mechanism predicts fractional kinetic orders for two different situations: if the two couples involved are electrochemically irreversible and their current-potential curves are in the Tafel region at the mixture potential E_{mix} ,²⁷ or if the two couples are reversible and E_{mix} lies in the steeply rising portions of the two current-potential curves.²⁸ The latter case can be ruled out because the reaction was not diffusion-controlled. In the former case the exponents should sum to unity for reaction (I). The exponents in eqn. (10) could just fit this requirement within the large experimental uncertainties.

The unexpectedly high catalytic rate obtained in run 10, in which Ce³⁺ ions were added to the reaction mixture, is discussed below.

Electrochemical Experiments with the Oxidised Surface

The quasi-steady-state current-potential curves for cerium solutions in 1 mol dm⁻³ HClO₄ on oxidised platinum surfaces were identical to those on the reduced platinum disc. This is not surprising, since the equilibrium potential of the solution is high enough to oxidise platinum, so that the surface was invariably in the oxidised state whatever the preconditioning employed. This was confirmed by the platinum oxide reduction peak obtained when a pre-reduced platinum disc, which had been in contact with a cerium solution, was swept cathodically.

Although the current-potential curves for solutions of Hg₂²⁺ and Hg²⁺ in 1 mol dm⁻³ HClO₄ on reduced platinum had displayed considerable hysteresis (Fig. 2), this was not observed on oxidised platinum (Fig. 6), where the surface remained in the oxidised state throughout. On the hypothesis of Wagner and Traud^{24,25} that the curves are additive when the cerium and mercury couples are present together, a mixture potential E_{mix} of ca. 0.66 V vs. NaSCE was predicted. This is similar to the initial potentials E_{cat} taken up by the catalysing disc in the first four runs in Table 3. However, this mixture potential lies in the limiting current region of the

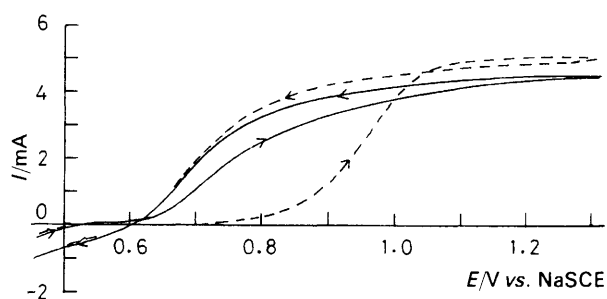


Fig 6 Current-potential curves of Hg^I-Hg^{II} solutions in 1 mol dm⁻³ HClO₄ at 25 °C taken at a rotation speed of 9 Hz and a sweep rate of 10 mV s⁻¹. The full curves refer to a solution 0.458 mmol dm⁻³ Hg₂²⁺ + 0.047 mmol dm⁻³ Hg²⁺ at a pre-oxidised platinum disc, the dashed curves to a solution of 0.512 mmol dm⁻³ Hg₂²⁺ and 0.051 mmol dm⁻³ Hg²⁺ at the disc immediately after finishing run 1 (Table 3)

Ce^{IV} reduction curve so that the catalysis should have been diffusion-controlled, which was not the case. Moreover, the predicted catalytic rate as calculated from the mixture current I_{mix} by eqn. (8) was some four times larger than the experimental rate.

The reason for this difference was investigated by voltammetric sweeps of the disc after the end of run 4 (Table 3). The disc was first rinsed with distilled water, immersed in 0.1 mol dm⁻³ HClO₄ solution and then connected to the potentiostat at 0.55 V. The potential was swept down to 0.0 V and then up to 1.8 V, and back again to 0.0 V and so on, as in the standard cleaning procedure. The full curve in Fig. 7, which represents the first sweep, shows an initial peak at around 0.22 V due to the reduction of platinum oxide. This proves that the surface remained in an oxidised state throughout the catalytic reaction, as would be expected from the high catalyst potentials. However, in the second and subsequent sweeps this peak shifted to ca. 0.30 V, suggestive of a change in the condition of the oxide. The second main feature in Fig. 7 is the appearance of an oxidation peak at ca. 0.98 V in the first anodic sweep, a peak which has disappeared in the second anodic sweep to be replaced by the gradual rise typical of platinum oxide formation. Following the arguments in connection with the reduced surface and the evidence in the literature,^{15,26} this peak may be assigned to the

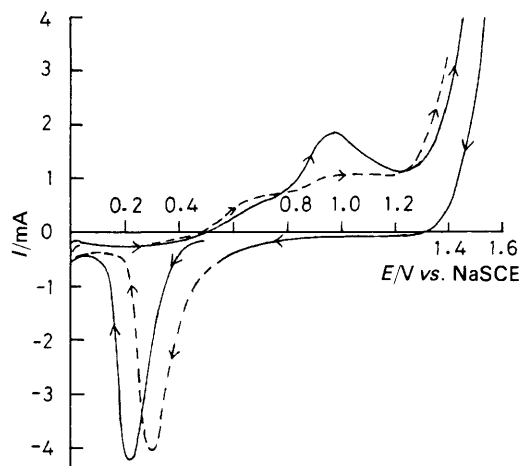


Fig. 7 Voltammetric sweeps of the platinum disc taken immediately after finishing run 4 in Table 1, in 0.1 mol dm⁻³ HClO₄ at 25 °C at a rotation speed of 6 Hz and a sweep rate of 50 mV s⁻¹. The full curve represents the first sweep and the dashed curve the second sweep

oxidative desorption of mercury deposited on the surface. The position of the peak was, however, more anodic by *ca.* 0.08 V than was found on reduced platinum electrodes. Its area was also smaller on the oxidised surface, and corresponded to the formation of only 1.0₄ monolayers of mercury. The exact nature of the mercury deposit on the oxidised platinum surface is not known, nor whether it alters the structure of the underlying layer.

The deposition of mercury helps to explain another aspect of the catalytic runs, the large rise in potential with time. The potential of the disc in the reaction mixture typically rose by *ca.* 0.01 V in <1 min, by over 0.04 V in the first 5 min and by 0.13–0.14 V in the first 2 h. This was qualitatively consistent with the changed electrochemical behaviour of the mercury couple. After the end of run 1 in Table 3, the disc was rinsed with distilled water, immersed in a fresh Hg^I–Hg^{II} solution in 1 mol dm⁻³ HClO₄, and the current–potential curves were determined. As Fig. 6 shows, the current of the anodic sweep rose much more slowly than before. If this curve is combined with that for the cerium couple, it leads to an *E*_{mix} value some 0.20 V higher than before. The cathodic sweep, on the other hand, was similar to that on a freshly prepared oxide surface because any mercury deposit will have been oxidatively desorbed. A massive hysteresis is thus apparent in the current–potential curves of the mercury couple on an electrode previously used in a catalytic run.

The cerium couple was less affected by the mercury deposit. The current–potential curves of a solution of 1 mmol dm⁻³ Ce^{IV} and 0.4 mmol dm⁻³ Ce³⁺ in 1 mol dm⁻³ HClO₄ were hardly changed when they were determined with a disc which had been immersed in a solution of 2.5 mmol dm⁻³ Hg₂²⁺ and 0.29 mmol dm⁻³ Hg²⁺ in 1 mol dm⁻³ HClO₄ for 1 min and then rinsed. A similar result was obtained when the curves were determined with a disc which had been immersed for 1 min in a typical reaction mixture (*cf.* runs 1–4 in Table 3) and then rinsed. Yet a change in the cerium current–potential curve must have occurred in order to produce the low catalytic rate, the absence of diffusion control and the kinetics observed in eqn. (10).

A significant clue is provided by run 10 in Table 3. Here 0.255 mmol dm⁻³ Ce³⁺ had been added to the reaction mixture, an addition which should have either had little or no effect²⁷ or else decreased the rate.²⁸ In fact, the catalytic rate rose by 42%! In the cyclic voltammetric scans carried out after this run the mercury oxidation peak was absent, showing that the Ce³⁺ ions (known to be adsorbed strongly on oxidised platinum²¹) had removed the mercury from the surface. It would thus appear that mercury ions adsorbed on the oxidised platinum disc had repelled Ce^{IV} ions, thereby lowering the rate of their electrochemical reduction. This would have altered the position and shape of the Ce^{IV}/Ce³⁺ current–potential curve in the reaction mixture. If addition of the appropriately modified curves of both the cerium and the mercury couples were to give a mixture potential at a point where both curves are in their Tafel region, the observed kinetics could be understood.²⁷ This is a further example of the way in which one couple can affect the electrochemical behaviour of another.²⁵

On the available evidence, therefore, we postulate the presence of *two* types of mercury species on the platinum oxide surface. The more firmly held mercury can be removed by reduction to Hg⁰ and subsequent electro-oxidation (Fig. 7). This mercury species is at least partly responsible for the rise in the catalyst potential during a run, for the slow decrease in catalytic rate with time and for the lower rate in a second run on the same disc (run 7 in Table 3). The second type of mercury on the surface would appear to be easily desorbed and removed by rinsing. Subsequent cerium current–

potential curves are thus little changed. This mercury species is likely to be Hg₂²⁺ rather than Hg²⁺.²⁶ These adsorbed ions then repel Ce^{IV} ions and so substantially decrease the catalytic rate of reaction (I). Both types of mercury species can be desorbed by added Ce³⁺ ions, which are strongly adsorbed on oxidised platinum surfaces.²¹

Kinetic and Electrochemical Experiments with a Partially Oxidised Surface

The structure and catalytic effectiveness of the oxidised disc were considerably changed on leaving it in contact with a solution of 5.01 mmol dm⁻³ Hg₂²⁺, 0.52 mmol dm⁻³ Hg²⁺ and 1 mol dm⁻³ HClO₄ at 25°C for 1 min before adding the cerium(IV) solution. The catalytic rate then increased by 44%, as run 11 in Table 3 shows. Contact between the oxidised disc and the mercury solution for 2 h before adding cerium(IV) increased the catalytic rate by 180% (run 12), to a value only 30% less than on a reduced platinum disc. This is easy to understand, for both thermodynamic considerations and electrochemical studies²⁶ show that the Hg₂²⁺ ions will have largely reduced the oxidised layer. Since the latter is believed to consist of adsorbed and place-exchanged hydroxyls,²⁹ we can write



This explanation was supported by the following electrochemical experiment. A freshly oxidised platinum disc was treated with a similar acid mercury solution for 1 min, rinsed and then scanned voltammetrically. As Fig. 8 shows, in the first cathodic sweep the peak for the platinum oxide reduction was much smaller than usual. This proves that much of the surface oxide had been removed by chemical reaction with Hg₂²⁺, as expressed by reaction (V). A reduction peak of normal size appears in the second cathodic sweep after the whole surface had been reoxidised. In the first anodic sweep a large peak appears at 0.92 V, which can clearly be attributed to oxidative desorption of mercury from the surface. This peak potential (in 1 mol dm⁻³ H₂SO₄) lies between the desorption potentials of 0.87 V observed for reduced platinum and 0.98 V found for oxidised platinum (in 0.1 mol dm⁻³ HClO₄, Fig. 7), consistent with much of the surface having been reduced. The peak area in Fig. 8 corre-

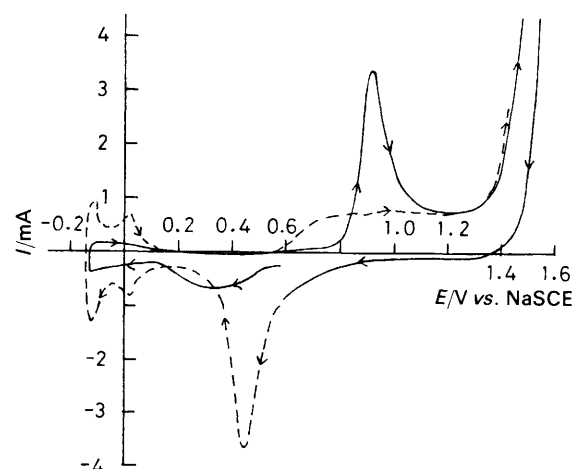


Fig. 8 Voltammetric sweeps of the platinum disc in 1 mol dm⁻³ H₂SO₄ at 25°C, at a rotation speed of 9 Hz and a sweep rate of 50 mV s⁻¹, after the disc had been in contact for 1 min with a solution of 5.01 mmol dm⁻³ Hg₂²⁺ and 0.52 mmol dm⁻³ Hg²⁺ in 1 mol dm⁻³ HClO₄. The full curve represents the first sweep and the dashed curve the second sweep

sponds to the desorption of 1.6_8 monolayers of mercury. This figure, too, lies between the values found for a reduced platinum surface after 1 min treatment with a mercury solution (2.3_3 monolayers) and for a completely oxidised surface (1.0_4 monolayers). The electrochemical evidence therefore supports the interpretation that treatment with a Hg_2^{2+} solution reduces the hydroxyl coating on the platinum disc. Since reduced platinum catalyses reaction (I) much more strongly than oxidised platinum, the catalytic rate after Hg_2^{2+} treatment lies between the values for these two surfaces and increases the longer the disc has been exposed to Hg_2^{2+} .

We thank the British Council and CONICIT, Venezuela, for financial support to J.M.G.M.

References

- Part 24.—A. M. Creeth and M. Spiro, *J. Chem. Soc., Faraday Trans.*, 1991, **87**, 977.
- P. L. Freund and M. Spiro, *J. Chem. Soc., Faraday Trans. 1*, 1983, **79**, 491.
- L. G. Sillén and A. E. Martell, *Stability Constants of Metal-Ion Complexes*. The Chemical Society, London, 1964, p. 44; H. G. Offner and D. A. Skoog, *Anal. Chem.*, 1966, **38**, 1520.
- J. M. Garnica Meza and M. Spiro, *Inorg. Chim. Acta*, 1991, in the press.
- Standard Potentials in Aqueous Solutions*, ed. A. J. Bard, R. Parsons and J. Jordan, Marcel Dekker, New York, 1985.
- H. B. Herman and J. R. Rairden, in *Encyclopedia of Electrochemistry of the Elements*, ed. A. J. Bard, Marcel Dekker, New York, 1976, vol. VI, pp. 45–48.
- P. K. Wrona and Z. Galus, in *Encyclopedia of Electrochemistry of the Elements*, ed. A. J. Bard, Marcel Dekker, New York, 1982, vol. IX, part A, pp. 32–34 and 64–74.
- M. Spiro, in *Comprehensive Chemical Kinetics, Vol. 28: Reactions at the Liquid-Solid Interface*, ed. R. G. Compton, Elsevier, Amsterdam, 1989, ch. 2.
- A. B. Ravnö and M. Spiro, *J. Chem. Soc.*, 1965, 97.
- J. Casado, A. Arrizabalaga and F. Andrés-Ordax, *Anal. Quim.*, 1971, **67**, 217.
- V. G. Levich, *Physicochemical Hydrodynamics*, Prentice-Hall, Englewood Cliffs, NJ, 1962, p. 69.
- J. Newman, *J. Phys. Chem.*, 1966, **70**, 1327.
- G. F. Smith and W. H. Fly, *Anal. Chem.*, 1949, **21**, 1233.
- R. Belcher and T. S. West, *Anal. Chim. Acta*, 1951, **5**, 260; 1952, **7**, 470.
- M. Z. Hassan, D. F. Untereker and S. Bruckenstein, *J. Electroanal. Chem.*, 1973, **42**, 161.
- M. Spiro and J. M. Garnica Meza, *Anal. Chim. Acta*, 1991, **242**, 279.
- J. B. Lee, *Corrosion (N.A.C.E.)*, 1981, **37**, 467.
- J. Topping, *Errors of Observation and Their Treatment*, Chapman & Hall, London, 4th edn., 1979, ch. 3.
- A. L. Horvath, *Handbook of Aqueous Electrolyte Solutions*, Ellis Horwood, Chichester, 1985, ch. 2.14.
- R. Haase and K-H. Dücker, *Z. Phys. Chem. N.F.*, 1965, **46**, 140.
- R. Greef and H. Aulich, *J. Electroanal. Chem.*, 1968, **18**, 295.
- M. Spiro and A. M. Creeth, *J. Chem. Soc., Faraday Trans.*, 1990, **86**, 3573.
- M. Sluyters-Rehbach and J. H. Sluyters, *Recl. Trav. Chim. Pays-Bas*, 1964, **83**, 983.
- C. Wagner and W. Traud, *Z. Elektrochem.*, 1938, **44**, 391.
- M. Spiro, *Chem. Soc. Rev.*, 1986, **15**, 141.
- S. Bruckenstein and M. Z. Hassan, *Anal. Chem.*, 1971, **43**, 928.
- M. Spiro, *J. Chem. Soc., Faraday Trans. 1*, 1979, **75**, 1507.
- P. L. Freund and M. Spiro, *J. Chem. Soc., Faraday Trans. 1*, 1983, **79**, 481.
- J. B. Benziger, F. A. Pascal, S. L. Bernasek, M. P. Soriaga and A. T. Hubbard, *J. Electroanal. Chem.*, 1986, **198**, 65.

Paper 0/04796A; Received 24th October, 1990